

Alpine lake optical properties as sentinels of dust deposition and global change

N. Mladenov,^{a,b,*} J. López-Ramos,^a D. M. McKnight,^b and I. Reche^{a,c}

^aDepartamento de Ecología, Universidad de Granada, Granada, Spain

^bInstitute for Arctic and Alpine Research, University of Colorado, Boulder, Colorado

^cInstituto del Agua, Universidad de Granada, Granada, Spain

Abstract

We characterized dissolved organic matter in La Caldera, an alpine lake in Sierra Nevada (Spain), and water-soluble organic compounds (WSOC) in dry and wet deposition originating from Saharan and marine air masses using ultraviolet–visible absorbance and three-dimensional fluorescence spectroscopy. Molar absorption coefficients at 250 and 280 nm in the lake were highly correlated with those in organic aerosol deposition, originating mainly from Saharan dust, and suggest that absorption in clear alpine lakes in unvegetated catchments may represent a unique sentinel of desertification and global change. Using parallel factor analysis modeling to resolve dominant fluorescent components, we identified a semiquinone-like fluorophore (C9) in the WSOC of deposition that was traced into the lake. At least three fluorescent components, including C9, contributed significantly to absorption of WSOC from atmospheric deposition. Saharan dust supplied chromophoric, aromatic, and fluorescent organic matter to this alpine lake. In contrast, marine organic aerosols had lower absorption coefficients, lower fluorescence intensity, and more microbial fluorescence properties.

Processes associated with global change, such as desertification and land use change, are promoting an increase in dust content in the atmosphere that has been particularly accentuated in recent decades (Prospero and Lamb 2003; Moulin and Chiapello 2006; Neff et al. 2008). The resulting increase in dust deposition has important chemical and biological effects on aquatic ecosystems (Duce and Tindale 1991; Morales-Baquero et al. 2006). For instance, dust deposition has been found to be an important source of nutrients (nitrogen and phosphorus) and other elements to alpine lakes and has been shown to have a fertilizing effect on alpine lake biota (Baron et al. 2000; Pulido-Villena et al. 2008; Reche et al. 2009).

Although the influence of mineral aerosols on aquatic ecosystems has been addressed, the role of organic aerosol inputs to lake ecosystems is a potentially important process but largely unexplored. Two lines of evidence underline the significant contribution of atmospheric inputs as a source of terrestrial organic matter into remote alpine lakes. First, lakes located on rocky terrain without vegetated catchments (e.g., Lake La Caldera in the Sierra Nevada, Spain) showed enriched $\delta^{13}\text{C}$ values of particulate organic matter that suggested a terrestrial origin likely derived from atmospheric inputs (Pulido-Villena et al. 2005). Second, water-soluble organic compounds (WSOC) in dust deposition were found to exert important effects on dissolved organic carbon concentration ([DOC]) and dissolved organic matter (DOM) optical properties in this alpine lake (Mladenov et al. 2008). In particular, ultraviolet–visible (UV-vis) absorbance analyses revealed that both dry and wet deposition supplied the lake with chromophoric DOM (CDOM). Because CDOM is photoprotective, acting to attenuate UV light in the water column, it is especially important for alpine lake biota, mostly for the more vulnerable bacterioplankton (Sommaruga et al. 1997;

Alonso-Saez et al. 2006). Furthermore, the humic fraction of DOM persists through time and, thereby, has the potential to be tracked by spectroscopic techniques and to provide useful information about changes in the lake ecosystem.

Fluorescence spectroscopy has successfully identified humic-like substances in WSOC in wet deposition (Kieber et al. 2006) and in high-volume active collectors (Duarte et al. 2004; Krivácsy et al. 2008). Three-dimensional excitation–emission matrices (EEMs) of aerosol WSOC contain distinct humic and protein peaks (Duarte et al. 2004), resembling those of aquatic DOM. Similarly, Kieber et al. (2006) showed that wet deposition contained CDOM and fluorescent compounds, with peaks in EEMs attributed to both terrestrial and marine DOM sources. Although dry deposition is known to be responsible for about 80% of total particulate matter (PM) deposition in the southwest Mediterranean region (Morales-Baquero et al. 2006), the fluorescent properties of WSOC in dry deposition have not been characterized.

To obtain quantitative information regarding the sources and redox state of DOM, parallel factor analysis (PARAFAC) has been successfully applied in fluorescence spectroscopy (Stedmon et al. 2003; Cory and McKnight 2005). With PARAFAC, EEMs are mathematically and statistically resolved, and the individual fluorescent components that produce these spectra are identified (Stedmon et al. 2003). A PARAFAC model of a large data set of DOM from diverse environments (Cory and McKnight 2005) identified important redox-active fluorescent components associated with quinones in various redox states as well as tyrosine and tryptophan-like fluorescent components. This approach for DOM characterization has advantages over more time-intensive and costly analyses, such as gas chromatography–mass spectroscopy, that identify only <20% of the organic compounds in aquatic or aerosol samples (Jacobson et al. 2000). Thus far,

* Corresponding author: mladenov@colorado.edu

PARAFAC modeling of fluorescence spectra has been useful in resolving DOM sources and reactivity in surface water (Mladenov et al. 2007; Wedborg et al. 2007) and groundwater studies (Banaitis et al. 2006; Mladenov et al. 2008) and has the potential to provide new insights for atmospheric and aquatic studies.

Here we hypothesize that dust deposition can be tracked in clear alpine lakes in unvegetated catchments via spectroscopic properties, absorbance, and fluorescence, and that changes in these properties can signal the current increasing dust deposition linked to global change. Our approach was to describe the spectroscopic character of WSOC in atmospheric deposition and to trace absorbance and fluorescent components from dust deposition to La Caldera, an oligotrophic alpine lake in the Sierra Nevada (Spain). We analyzed absorbance and fluorescence properties, including a distribution of PARAFAC components in DOM from La Caldera and WSOC from atmospheric deposition. To evaluate the contribution of fluorescent components from end members, we also examined fluorescence properties of WSOC from Sahara Desert and La Caldera soils.

Methods

Sample collection—Water samples were collected weekly during the ice-free period of 2007 from near the center and surface of La Caldera (maximum lake depth ~10 m). All DOM samples were transported chilled to the laboratory, where they were filtered through precombusted (>2 h at 500°C) Whatman GF/F filters and stored in precombusted amber glass bottles at approximately 4°C in the dark until analysis. Samples collected for DOC analysis were preserved by acidifying to a pH of about 2 with concentrated HCl or H₃PO₄.

Separate samples of dry and wet deposition were collected every 2 weeks during the ice-free period of 2007 from 21 June to 24 October using a MTX1 ARS 1010 automatic deposition sampler located at 2900 m above sea level (asl) (37.03°N, 3.23°W) near the study lake. More details on atmospheric sample collection can be found elsewhere (Morales-Baquero et al. 2006).

PM and WSOC analyses—PM loadings (mg m⁻² d⁻¹) were obtained by rinsing the dry-deposition receptacle with 1 liter of high-quality ultrapure MilliQ water. For wet deposition, the volume of rain in the receptacle was recorded and a 1-liter aliquot was used for analyses. If the rain volume was less than 1 liter, it was brought up to that volume with ultrapure MilliQ water (Pulido Villena et al. 2006). For dry and wet deposition, approximately 500 mL of the suspension was filtered through precombusted and preweighed Whatman GF/F filters. The filters were dried at 50°C for >24 h and reweighed to determine the PM loading. The filtrates, referred to as the WSOC, were stored in precombusted amber glass bottles at approximately 4°C in the dark until analysis. All samples were acidified to a pH of about 2 with concentrated HCl or H₃PO₄. DOC concentrations of WSOC samples were normalized to the volume of MilliQ water used, area of the bucket, and collection period to determine the WSOC

loading (mg m⁻² d⁻¹). Before UV-vis absorbance and fluorescence analyses, WSOC samples were brought to an ambient pH of between 6 and 7 (comparable with wet-deposition pH) with concentrated NaOH.

WSOC was extracted from two Saharan soil samples, collected from Mauritania (sand A; 19°00.193'N, 16°11.214'E) and Western Sahara (sand B; 21°35.196'N, 16°55.124'E). Also, two local soil samples, one sample scraped from beneath rocks within 5 m of the lake fringe and the other sample swept from the dusty layer on and between rocks, were collected from the watershed of La Caldera Lake. A ratio of 1 g of soil to 10 mL of high-quality MilliQ water (Kalbitz et al. 2003) was used for WSOC extraction and the suspensions were filtered through precombusted (2 h at 500°C) Whatman GF/F filters after agitating for 60 min on a shaker table. The pH of MilliQ water (between 6 and 7) is in the same range as the pH of La Caldera Lake water, to ensure that pH effects on solubility in the WSOC extractions would be similar to field conditions. Organic matter content was measured as loss on ignition by combusting 5 g of oven-dried soil at 550°C for 4 h (Heiri et al. 2001).

Laboratory analyses—[DOC] was measured on filtered-acidified lake water, soil WSOC, and dry- and wet-deposition WSOC samples within 3 months of collection using a Shimadzu TOC-V CSH equipped with a high-sensitivity catalyst. For lake and soil samples and dry- and wet-deposition WSOC samples, UV-vis absorbance and fluorescence were measured at field pH (between 6 and 7). UV-vis absorbance scans were measured within a month of collection at a range of 250–900 nm for all samples, except for two Saharan soil samples (range 200–700 nm), in 10-cm path length quartz cuvettes using a Perkin Elmer Lambda 40 spectrophotometer connected to a computer equipped with UV-Winlab software. The absorbance value at 690 nm was used to correct UV absorbance values for scattering (Laurion et al. 2000). Absorbance at 250 nm and 320 nm wavelengths were expressed as Napierian absorption coefficients (a_{250} and a_{320}) and were calculated by multiplying the absorbance values by 2.303 and dividing by the optical path length in meters. The molar absorption coefficients (m² mol⁻¹) at 250 nm (ϵ_{250}), 280 nm (ϵ_{280}), and 320 nm (ϵ_{320}) were calculated by dividing the absorption coefficients by the [DOC] in millimoles per liter. The molar absorption coefficient at wavelengths between 250 and 280 nm, where aromatic moieties absorb most strongly, is often used to evaluate the contributions of vascular plant sources and organic soil to the DOM pool (Chin et al. 1994; Weishaar et al. 2003). Values are also reported for 320 nm, a wavelength commonly used to refer to color, and a_{320} is often taken as a surrogate for UV attenuation in the water column (Morris et al. 1995; Laurion et al. 2000). We refer to absorption at 250 nm and 320 nm as a measure of aromaticity and color, respectively.

Fluorescence spectroscopy has provided valuable insights into the sources of DOM in aquatic samples from the generation of EEMs (Coble 1996), determination of the fluorescence index (FI; McKnight et al. 2001), and PARAFAC modeling (Stedmon et al. 2003). EEMs are a three-dimensional representation of fluorescence intensities

scanned over a range of excitation:emission (Ex:Em) wavelengths. Prominent humic peaks have been found in EEMs, one stimulated by UV excitation (at Ex:Em 240–260:380–460 nm) and another stimulated by visible excitation (at 320–350:420–480 nm). Other peak areas are attributed to tyrosine and tryptophan amino acid fluorescence at 275:310 nm and 275:340 nm (Coble 1996). EEMs were measured using a JY-Horiba Spex Fluoromax-3 spectrophotometer and were scanned using an integration time of 0.25 s over an excitation range of 240–450 nm at 10-nm increments (and later interpolated to 5-nm increments) and an emission range of 350–550 nm at 2-nm increments. To correct for lamp spectral properties and to be able to compare with fluorescence reported in other studies, spectra were collected in signal:reference mode and instrument-specific excitation and emissions corrections were applied. Corrections and generation of EEMs were performed using MATLAB. MilliQ water blanks were subtracted to remove Raman scattering and all samples were normalized to the Raman area to account for lamp decay over time. Because of the low [DOC] and absorbance of lake and deposition samples, no inner-filter effect correction was applied.

EEMs of lake DOM and dry- and wet-deposition WSOC were fit to the PARAFAC model of Cory and McKnight (2005) that identified 13 individual components responsible for fluorescence, and the relative amount (percentage of total) of each component was measured. Model fit was considered suitable if intensities in the residual, generated by subtracting the PARAFAC-modeled EEM from the measured EEM, were within 10% of measured intensities. An EEM of a MilliQ water blank, submitted to the same sample handling and processing as lake samples, did not show any residual peaks when fit to the PARAFAC model. Three lake samples that were acidified and later neutralized showed the same EEMs as unacidified samples. The distribution of PARAFAC components was also similar, with <2% change in any component, with the exception of C13, which increased 3.2% in one lake sample after acidification and subsequent neutralization.

Of the 13 components identified by PARAFAC, there are three components with fluorescence maxima positions similar to oxidized quinones (Q) (C2, C11, and C12); four similar to reduced semiquinones (SQ) and a hydroquinone (HQ) (C5, C7, C9, and C4); and two amino acid-like components similar to tryptophan and tyrosine (C8 and C13, respectively) (Cory and McKnight 2005). Here we report the total fluorescence loading in Raman units (RU) and the relative contribution of each component to the total fluorescence (percentage) as in Stedmon et al. (2003). We also report molar fluorescence values (e.g., f_{total} , f_{C9}), which are calculated as the fluorescence loading normalized to the DOC concentration. The redox index (RI) (Miller et al. 2006) provides information about the redox state of quinone-like components obtained from PARAFAC modeling and is defined as the ratio of reduced quinone-like components to total quinone-like components.

The FI (McKnight et al. 2001) was obtained from corrected EEMs at an excitation of 370 nm and the ratio of intensities emitted at 470:520 nm (Cory and McKnight

2005) with a confidence interval of 0.01. Among samples, collected over time from the same system and analyzed with the same instrument with appropriate corrections, changes in FI of 0.05 have been found to indicate shifts in dominant DOM source (Hood et al. 2003). Two semiquinone-like fluorescent components are known to be responsible for the FI (C5 and C7) (Cory and McKnight 2005), and when there is little or no fluorescence at higher excitation wavelengths the two-dimensional FI spectra are influenced by other more dominant components. Therefore, in samples with low amounts of C5 or little or no fluorescence above 320 nm, the FI was calculated from the equation of the significant relationship between FI and C5 and C7 proposed by Cory and McKnight (2005):

$$\text{FI} = -1.2(\text{C5}/[\text{C5} + \text{C7}]) + 2.0 \quad (1)$$

Data analyses—To test for significant correlations between parameters, linear regressions and bivariate correlations were performed using Statistica software.

We examined the source of air masses over the Sierra Nevada, Spain (37.3°N, 3.19°W) by computing daily backward trajectories (<http://www.arl.noaa.gov/ready.html>) using the HYSPLIT model (Draxler and Rolph 2003) and archived data from the Global Data Assimilation System data set with 120 h of run time. We also consulted summary data of aerosol episodes at surface elevation in the southeast Spain region (<http://www.calima.ws>) and vertical profiles of dust concentration (<http://www.bsc.es/projects/earthscience/DREAM>) at the Granada site (37.16°N, 3.61°W). Precipitation data for the study area were obtained from National Oceanic and Atmospheric Administration (NOAA) Climate Data Online (<http://cdo.ncdc.noaa.gov/CDO/cdo>) surface data, Global Summary for the Day, for the Granada airport station (08419099999). Daily backward trajectories were consulted to verify the source of air masses for each precipitation event.

To quantify the significance of atmospheric inputs of WSOC for the lake DOC budget, we performed a DOC mass balance calculation for the lake. We calculated the range of lake DOC mass by multiplying the minimum and maximum observed DOC concentrations by the total lake volume. The daily DOC mass transported into the lake and catchment by dry and wet deposition of WSOC was calculated by multiplying the mean areal WSOC deposition rate by the lake surface area and catchment surface area, respectively. The daily DOC deposited to the lake and catchment was represented as the fraction of the total DOC (percentage) by dividing by minimum and maximum lake DOC mass.

Results

Characterization of WSOC from dust deposition and Saharan soils—According to summary data of aerosol episodes, aerosols originated in northern Africa in 72 of 126 d during the sampling period. Backward trajectories suggest that the remainder was dominated by marine air masses originating over the Atlantic Ocean. Almost all sampling periods experienced Saharan dust events (Ta-

Table 1. Dust source information for each collection period and PM loading, absorption, and fluorescence properties of dry deposition.

Properties*	Saharan-dominated				Marine-dominated			
	01–14 Aug	15–28 Aug	29 Aug–11 Sep	Mean	18–31 Jul	27 Sep–09 Oct	10–24 Oct	Mean
Mean vertical dust concentration ($\mu\text{g m}^{-3} \text{d}^{-1}$) [†]	71 (0–230)	199 (0–840)	93 (0–770)	121	47 (0–200)	20 (0–180)	33 (0–130)	33
Backtraj-Saharan (d) [‡]	8	6	7	7	0	5	5	3
Backtraj-Marine (d) [‡]	4	5	3	4	14	9	8	10
PM loading ($\text{mg m}^{-2} \text{d}^{-1}$)	36.1	34.2	91.0	53.8	44.6	25.1	7.75	25.8
WSOC loading ($\text{mmol m}^{-2} \text{d}^{-1}$)	0.29	0.32	0.42	0.34	0.24	0.31	0.24	0.26
Absorption								
a_{250} (m^{-1})	8.35	3.90	4.73	5.65	1.54	3.70	2.76	2.67
a_{280} (m^{-1})	6.29	2.67	3.28	4.08	1.32	2.69	2.30	2.10
a_{320} (m^{-1})	1.11	0.65	0.79	0.85	0.44	0.54	0.53	0.50
ε_{250} ($\text{m}^2 \text{mmol}^{-1}$)	30.5	13.2	12.1	18.6	6.98	13.6	11.3	10.6
ε_{280} ($\text{m}^2 \text{mmol}^{-1}$)	23.0	9.05	8.37	13.5	5.97	9.88	9.41	8.42
ε_{320} ($\text{m}^2 \text{mmol}^{-1}$)	4.08	2.19	2.00	2.75	2.00	1.97	2.16	2.04
Fluorescence								
FI	1.34	1.30	1.34	1.33	1.46	1.51	1.42	1.46
Total loading (RU)	0.59	0.32	0.35	0.42	0.24	0.24	0.20	0.22
f_{total} (RU L mmol^{-1})	2.15	1.09	0.89	1.38	1.07	0.88	0.81	0.92
%C1	T	6.7	5.8	6.1	6.2	4.5	6.5	5.8
%C2 (Q2)	M	15	14	14	14	12	13	15
%C3	M	5.9	3.8	3.7	4.5	5.5	4.1	3.4
%C4 (HQ)	B	18	21	21	20	22	19	12
%C5 (SQ1) [§]	T	3.3	3.3	3.3	3.3	2.0	1.6	2.4
%C6	M	2.0	3.9	3.6	3.2	1.7	4.3	2.7
%C7 (SQ2)	M	2.9	2.5	3.0	2.8	2.4	2.7	2.8
%C8 (Trp)	M	7.2	12	11	10	13	7.9	5.4
%C9 (SQ3)	M	4.8	3.2	2.9	3.6	2.1	2.7	2.9
%C10	T	11	9.1	7.6	9.1	5.3	10	7.5
%C11 (Q1)	T	8.6	4.8	6.7	6.7	5.5	5.0	15
%C12 (Q3)	M	12	12	12	12	14	13	11
%C13 (Tyr) [§]	M	3.5	3.9	5.1	4.2	8.9	9.5	13
%AAs		11	16	16	14	22	17	19
RI		0.44	0.49	0.48	0.47	0.47	0.46	0.32

* Backtraj, backward trajectory; PM, particulate matter; WSOC, water-soluble organic compounds; FI, fluorescence index; f_{total} , total molar fluorescence; RI, redox index. The molecular association of components (Cory and McKnight 2005) is defined as: M, microbial; T, terrestrial; B, associated with both microbial and terrestrial DOM sources; Q, quinone-like; SQ, semiquinone-like; HQ, hydroquinone-like; Trp, tryptophan-like; Tyr, tyrosine-like; AAs, amino acid-like components (C8 + C13).

[†] Two-week mean, derived from BSC (2008). Range (minimum–maximum concentrations) shown in parentheses.

[‡] Summed over the 2-week collection period.

[§] Indicates significant difference (by two-tailed heteroscedastic *t*-test; *p*-level <0.01) between components in Saharan- and marine-dominated samples.

ble 1). However, some periods received noticeably higher amounts of dust at 3000 m and were dominated by Saharan air masses (Saharan-dominated), while others had low dust concentrations and were dominated by marine air masses (marine-dominated) (Table 1; Fig. 1). Three sampling periods were not definitively discerned as either Saharan- or marine-dominated and are not included in Table 1, although their spectroscopic properties were included in this study. All rain events were associated with Saharan air masses, except for the 29 September 2007 event (Table 2).

In dry deposition (Table 1), the PM loading ranged from 7.75 to 91.0 $\text{mg m}^{-2} \text{d}^{-1}$ and the WSOC loading ranged from 0.24 to 0.42 $\text{mmol m}^{-2} \text{d}^{-1}$, representing on average 15% of the PM dry deposition. The range of a_{250} was from 1.54 to 8.34 m^{-1} and ε_{250} ranged from 6.98 to

30.5 $\text{m}^2 \text{mol}^{-1}$ (Fig. 2). For both a and ε , the highest and lowest values appeared during a Saharan-dominated event (01–14 August) and a marine-dominated event (18–31 July 2007), respectively. The loading of PM was not substantially different among these two periods (Table 1). The absorption spectra of the 01–14 August dry deposition sample had a peak at 285 nm, whereas those of the 29 August–11 September wet and 18–31 July dry periods were less intense at all wavelengths and relatively featureless, with a shoulder centered at 260 nm (Fig. 3A). FI values were low (ranging from 1.30 to 1.51) for all WSOC samples (Fig. 2). RI values were high and ranged from 0.44 to 0.49, with one outlier value (0.32) recorded for the period of 10–25 October 2007.

In wet deposition, the PM loading ranged from 5.32 to 106.4 $\text{mg m}^{-2} \text{d}^{-1}$ (Table 2) and the WSOC loading tracked

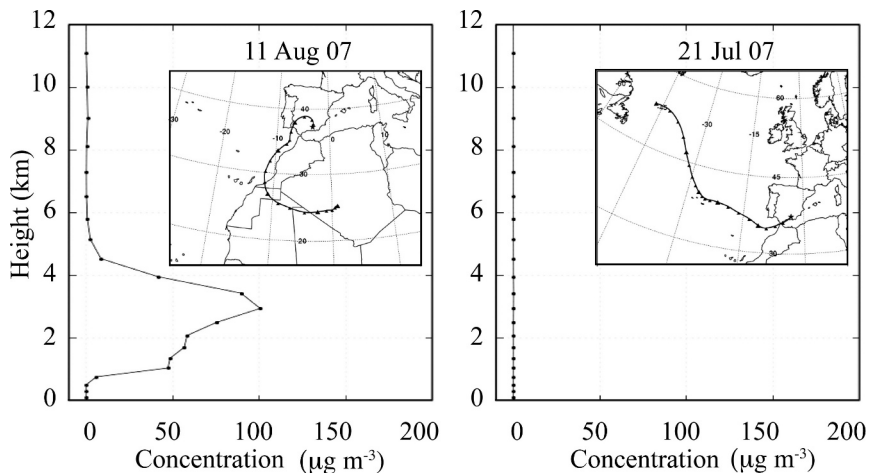


Fig. 1. Vertical dust concentration profiles (source: Barcelona Supercomputing Center) for dates with Saharan (left) and marine (right) air mass sources and sample 5-d backward trajectories (source: NOAA READY website) ending at 00:00 h coordinated universal time for each date (inset). The location of the Sierra Nevada site (3000 m asl and 37.3°N, 3.19°W) is designated with a star in the backward trajectories.

Table 2. Rainfall information, wet PM loading, absorption, and fluorescence properties during collection periods with wet deposition.

Properties*	15–28 Aug	29 Aug–11 Sep	12–26 Sep	27 Sep–09 Oct	10–24 Oct	Mean
Dates with rain events	26 Aug ^S	11 Sep ^S	21 Sep ^S , 22 Sep ^S	29 Sep ^M , 03 Oct ^S , 05 Oct ^S	15 Oct ^S , 16 Oct ^S	
PM loading (mg m ⁻² d ⁻¹)	93.0	106.4	39.5	17.5	5.32	52.3
WSOC loading (mmol m ⁻² d ⁻¹)	0.08	0.31	0.11	0.10	0.06	0.13
Absorption						
a_{250} (m ⁻¹)	3.05	3.73	—	3.09	—	3.29
a_{320} (m ⁻¹)	1.86	2.51	—	2.04	—	2.14
a_{320} (m ⁻¹)	0.74	1.12	—	0.94	—	0.93
ϵ_{250} (m ² mmol ⁻¹)	41.3	12.8	—	7.70	—	20.6
ϵ_{250} (m ² mmol ⁻¹)	25.1	8.60	—	5.09	—	12.9
ϵ_{320} (m ² mmol ⁻¹)	9.95	3.83	—	2.34	—	5.38
Fluorescence						
FI	1.43	1.46	1.31	1.58	—	1.45
Total loading (RU)	0.46	0.52	0.37	0.35	—	0.42
f_{total} (RU L mmol ⁻¹)	6.2	1.8	3.6	0.87	—	3.1
%C1	T	5.7	5.7	4.3	—	5.5
%C2 (Q2)	M	13	15	12	16	14
%C3	M	5.3	4.3	5.1	6.0	5.2
%C4 (HQ)	B	20	20	20	13	18
%C5 (SQ1)	T	2.1	2.8	1.7	0.9	1.8
%C6	M	3.3	5.7	4.5	8.4	5.5
%C7 (SQ2)	M	3.4	3.5	2.4	4.2	3.4
%C8 (Trp)	M	13	11	16	6.6	12
%C9 (SQ3)	M	2.7	2.3	2.0	2.2	2.3
%C10	T	5.1	6.0	4.8	4.7	5.1
%C11 (Q1)	T	5.1	5.8	6.0	7.8	6.2
%C12 (Q3)	M	13	11	16	13	13
%C13 (Tyr)	M	8.2	6.7	5.5	10.5	7.7
%AAs		21	17	22	17	19
RI	0.48	0.47	0.43	0.35	—	0.43

* Backtraj, backward trajectory; ^S backward trajectory indicates Saharan air mass source for this date; ^M backward trajectory indicates marine air mass source for this date; PM, particulate matter; WSOC, water-soluble organic compounds; FI, fluorescence index; f_{total} , total molar fluorescence; RI, redox index. The molecular association of components (Cory and McKnight 2005) is defined as: M, microbial; T, terrestrial; B, associated with both microbial and terrestrial DOM sources; Q, quinone-like; SQ, semiquinone-like; HQ, hydroquinone-like; Trp, tryptophan-like; Tyr, tyrosine-like; AAs, amino acid-like components (C8 + C13); dash indicates missing data.

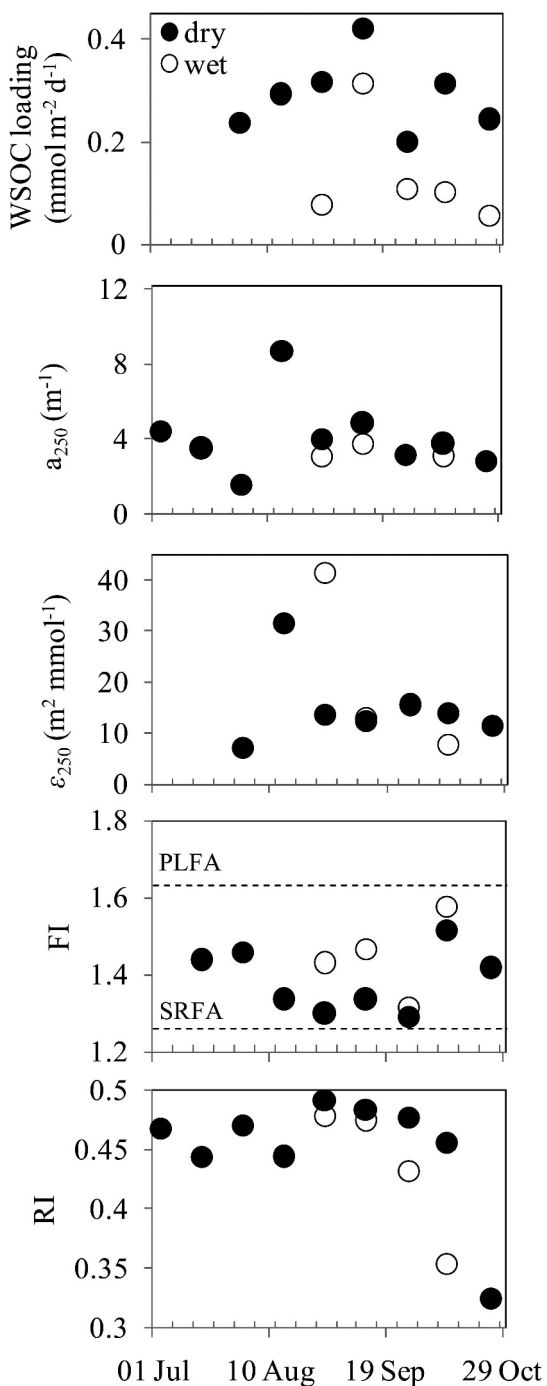


Fig. 2. Time series of WSOC concentration, absorption coefficient at 250 nm (a_{250}), molar absorption coefficient at 250 nm (ϵ_{250}), fluorescence index (FI), and redox index (RI) in dry (filled circles) and wet (empty circles) deposition. The FI values of microbial (Pony Lake Reference Fulvic Acid [PLFA]) and terrestrial (Suwannee River Reference Fulvic acid [SRFA]) end members are shown.

that of dry deposition (Fig. 2). Absorption and molar absorption values (Table 2) were similar to Saharan dry deposition values (Table 1) and, with the exception of the 15–28 August period, tracked dry deposition values closely

(Fig. 2). In general, FI values were higher and RI values were lower in wet deposition than in dry deposition (Fig. 2).

EEMs of Saharan-dominated dry and wet WSOC contained peaks typically found in aquatic humic substances, whereas those of marine-dominated WSOC lacked typical fluorescence peaks (Fig. 3B). For example, EEMs of Saharan-dominated dry WSOC showed prominent but blue-shifted peaks at approximately 240:425 nm and 305:425 nm, whereas these peaks were not visible in the EEMs of marine-dominated WSOC (Fig. 3B). Instead, the EEMs of marine-dominated WSOC had evident amino acid peaks (near 260–280:350 nm) and very low fluorescence intensity at excitation wavelengths >320 nm (Fig. 3B).

PARAFAC-modeled EEMs for dry and wet deposition were similar to measured EEMs and showed no large residual peaks, indicating that the model captured the real data (Table 1; Fig. 3B). The distribution of fluorescent components provided by PARAFAC showed that in all deposition samples, quinones (Q + SQ + HQ) were the most dominant fluorescent group, representing on average 63% and 59% of the total fluorescence loading in dry and wet deposition, respectively. The main differences among the EEMs of Saharan- and marine-dominated WSOC were in the amounts of amino acid-like components. Specifically, C13 (tyrosine-like) was significantly higher in marine-dominated dry deposition and C5 (a semiquinone-like component linked to terrestrial sources) was significantly higher in Saharan-dominated dry deposition (Table 1). Of all dry deposition samples collected, the amounts of amino acid-like components were highest in a marine-dominated sample (18–31 July) and lowest in a Saharan-dominated sample (01–14 August) (Table 1). The amount of amino acid-like components in wet deposition (Table 2) was higher than in Saharan-dominated dry deposition and similar to the amount observed in marine-dominated dry deposition (Table 1).

To evaluate which fluorescent components contributed most to absorption in total deposition, we examined relationships between all fluorescent components and absorption coefficients at 250, 280, and 320 nm. We found significant relationships between a_{320} and the fluorescent components C1 (an anomeric compound of microbial association) and C7 and C9 (two microbial semiquinones) (Table 3). These three components were higher in Saharan-dominated WSOC than in marine-dominated WSOC (Table 1). C9 was also significantly related to a_{250} and a_{280} (Table 3). The values of a_{250} , a_{280} , and a_{320} were significantly and negatively related to the content of amino acid-like components (Table 3). The total molar fluorescence (f_{total}) was significantly and positively related to molar absorption coefficients (Table 3).

We characterized the dust end member by examining the absorbance and fluorescence properties of two Saharan soils. Both soils contained low amounts of organic matter that can be lost to ignition (*see %OM*, Table 4) and leached during wetting (*see WSOC content*, Table 4). But molar absorption coefficients of the WSOC extracted from Saharan soils were higher than those measured in most atmospheric deposition samples. FI values were very high

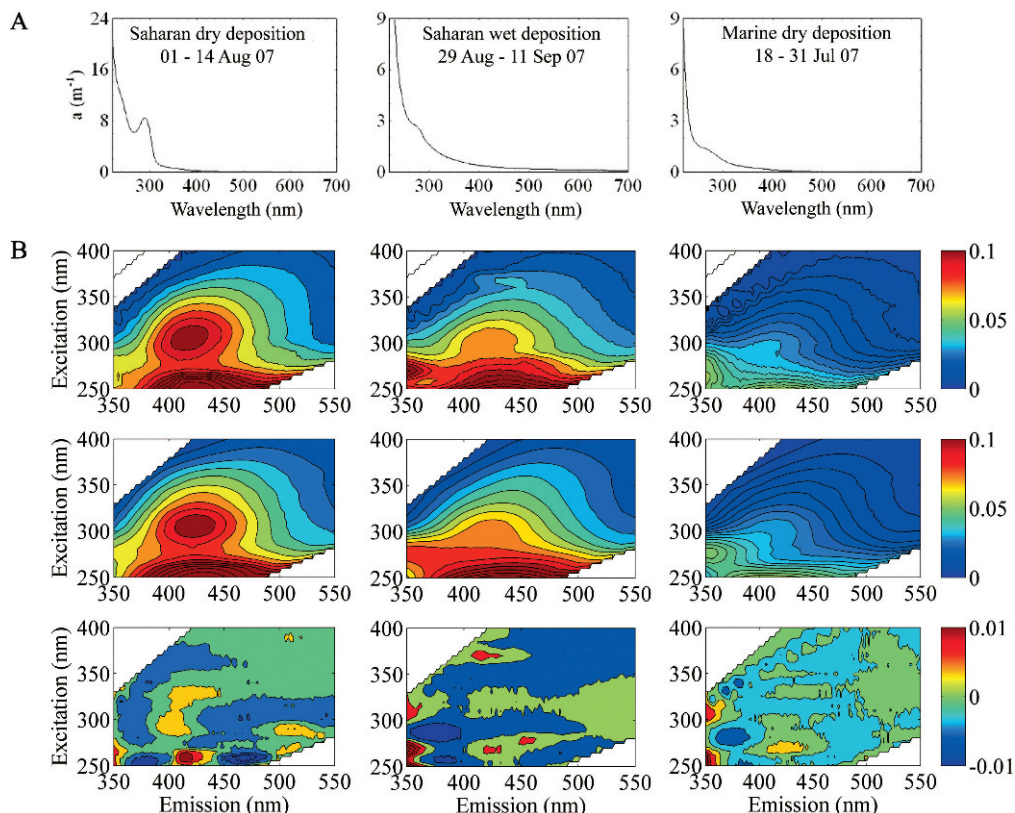


Fig. 3. (A) UV-vis absorption scans from 220–700 nm and (B) representative measured (top panels), PARAFAC-modeled (middle panels), and residual (bottom panels) excitation–emission matrices (EEMs) of deposition samples from sampling periods dominated by Saharan dry deposition (left), Saharan wet deposition (center), and marine dry deposition (right). Note the different scale for the Saharan dry-deposition UV-vis scan.

and the EEMs of soil leachates were most heavily dominated by amino acid-like fluorescence with peaks centered at between Ex 250–275 nm and Em 350–380 nm (Fig. 4). The distribution of PARAFAC components suggests that the combined tryptophan- and tyrosine-like components (C8 and C13) are the most dominant fluorescent components, representing >40% of the total fluorescence. PARAFAC-modeled EEMs underpredict the measured EEMs by more than 10% in these regions (Fig. 4); therefore, the combined tyrosine- and tryptophan-like fluorescence in Saharan soil WSOC may be even higher. Along with components C5, C6, and C10, C9 was

found in very low amounts (<2% of the total fluorescence) in WSOC extracted from these two Saharan soil end-member samples.

Lake DOM characterization and deposition effects on lake DOM—The [DOC] and absorption coefficients (a_{250} and a_{320}) in La Caldera ranged from 0.03 to 0.40 mmol L⁻¹ and from 0.94 to 4.64 m⁻¹ and 0.15 to 1.81 m⁻¹, respectively (Table 5, Fig. 5). The FI ranged from 1.53 to 1.64 and RI ranged from 0.37 to 0.47 (Table 5, Fig. 5).

A review of the residual lake EEMs showed that, with the exception of one residual peak at 300:380 nm

Table 3. Relationships (positive or negative relationships in parentheses) between absorption coefficients, relative amounts of fluorescent components, and total molar fluorescence (f_{total}) of the WSOC of total (wet+dry) deposition.

Properties	%C1	%C7	%C9	%AAs [†]	f_{total} (RU L mmol ⁻¹)
a_{250} (m ⁻¹)	(+)	(+)	(+) 0.37*	(-) 0.79**	(+)
a_{280} (m ⁻¹)	(+)	(+)	(+) 0.50*	(-) 0.89**	(+)
a_{320} (m ⁻¹)	(+) 0.52**	(+) 0.64**	(+) 0.53**	(-) 0.41*	(+)
ϵ_{250} (m ² mmol ⁻¹)	(+)	(+)	(+)	(-)	(+) 0.78**
ϵ_{280} (m ² mmol ⁻¹)	(+)	(+)	(+)	(-)	(+) 0.58**
ϵ_{320} (m ² mmol ⁻¹)	(+)	(+)	(+)	(-)	(+) 0.99**

[†] AAs, amino acid-like components (C8 + C13).

* $p < 0.05$; ** $p < 0.01$; R^2 values shown only for significant relationships.

Table 4. Organic matter (OM) content, absorption, and fluorescence properties of WSOC from two Saharan soils.

Properties*	Sand A	Sand B
Lat., long.	19°00.193'N, 16°11.214'E	21°35.196'N, 16°55.124'E
% OM (mg OC [g dry wt] ⁻¹)	0.33	0.42
WSOC content (mg DOC [g dry wt] ⁻¹)	2.1 × 10 ⁻³	2.3 × 10 ⁻³
Absorption		
<i>a</i> ₂₅₀ (m ⁻¹)	3.54	4.03
<i>a</i> ₂₈₀ (m ⁻¹)	2.51	2.92
<i>a</i> ₃₂₀ (m ⁻¹)	1.15	1.49
ε ₂₅₀ (m ² mmol ⁻¹)	99.9	103
ε ₂₈₀ (m ² mmol ⁻¹)	70.9	74.7
ε ₃₂₀ (m ² mmol ⁻¹)	32.5	38.2
Fluorescence		
FI	1.81	1.83†
Total fluorescence (RU)	0.52	0.40
<i>f</i> _{total} (RU L mmol ⁻¹)	21.6	19.9
%C1	T	7.0
%C2 (Q2)	M	14
%C3	M	2.7
%C4 (HQ)	B	18
%C5 (SQ1)	T	1.5
%C6	M	0.0
%C7 (SQ2)	M	8.0
%C8 (Trp)	M	19
%C9 (SQ3)	M	0.5
%C10	T	1.8
%C11 (Q1)	T	4.2
%C12 (Q3)	M	22
%C13 (Tyr)	M	2.3
%AAs		21
RI	0.41	0.47

* FI, fluorescence index; *f*_{total}, total molar fluorescence; RI, redox index. The molecular association of components (Cory and McKnight 2005) is defined as: M, microbial; T, terrestrial; B, associated with both microbial and terrestrial DOM sources; Q, quinone-like; SQ, semiquinone-like; HQ, hydroquinone-like; Trp, tryptophan-like; Tyr, tyrosine-like; AAs, amino acid-like components (C8 + C13).

† Calculated from the relationship of FI and C5: (C5 + C7) (Cory and McKnight, 2005).

(representing approximately 25% of the measured EEM intensity and found at approximately the same location and intensity in all lake EEMs), all residual EEMs were within 10% of the measured EEMs (Fig. 6). Among the components identified by the PARAFAC model, C2 (quinone-like), C3 (unknown), C4 (hydroquinone-like), and C12 (quinone-like) were the most dominant in La Caldera (Table 5). Quinone-like fluorescent components dominated the EEM distribution and represented between 61% and 68% of the total fluorescence. The amino acid-like components, C8 and C13, changed the most during the 2007 sampling season, ranging from 9% to 19% of the component distribution (Table 5).

The WSOC of dust recovered near the lake was different in absorption and fluorescence from a deeper soil sample collected near the lake. Molar absorption coefficients for this soil sample were lower than both lake and dust near the lake samples (Table 5). FI values for WSOC of soil near the lake were much higher than those for dust near the lake. The PARAFAC distribution for this soil should be interpreted with caution since the PARAFAC fit was not completely suitable, containing many peaks in the residual EEM >10% of the measured EEM intensity (Table 5).

Nevertheless, the EEM of soil near the lake was much different from most lake EEMs and the EEM of dust near the lake (Fig. 6). The EEM of dust near the lake was most similar to dry-deposition EEMs.

To evaluate whether atmospheric deposition provided substantial WSOC mass to influence lake DOM budget, we calculated the daily mass loading (6.1 × 10³ mmol d⁻¹ and 2.8 × 10³ mmol d⁻¹ of dry and wet deposition, respectively) of WSOC to the lake (Table 6). The range of DOC mass in the lake is 1.4 × 10⁶–5.6 × 10⁶ mmol; therefore, over the course of 1 month the total WSOC loading directly to the lake (8.9 × 10³ mmol d⁻¹) represents on average 6% of the total lake DOC mass. Deposition to the lake catchment (99 × 10³ mmol d⁻¹) represents 66% of the total lake DOC mass over a 1-month period.

The WSOC loading in total deposition was not significantly related to DOC concentration in La Caldera. However, ε₂₅₀ and ε₂₈₀ in La Caldera and in total deposition were significantly related (Fig. 7). Molar absorption coefficients were typically twice as high in La Caldera than in deposition. The amount of the microbial semiquinone-like fluorophore (C9) and its molar fluorescence were significantly correlated in lake and total deposition (Fig. 7).

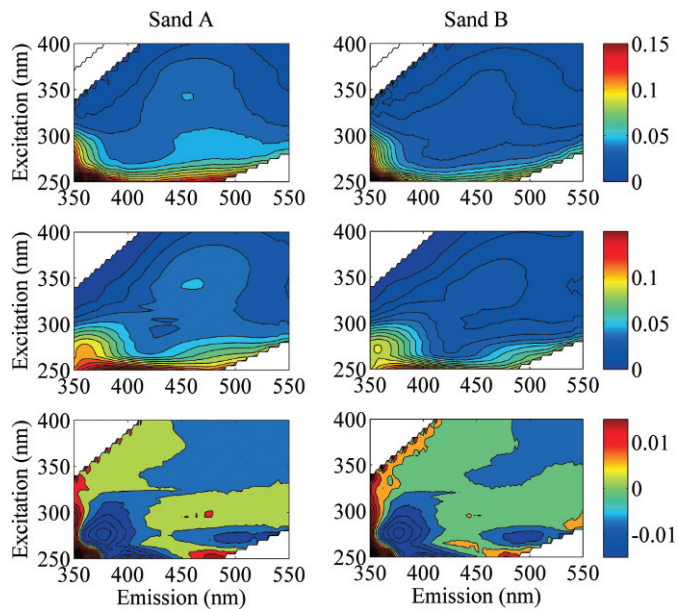


Fig. 4. Measured (top panels), PARAFAC-modeled (middle panels), and residual (bottom panels) excitation emission matrices (EEMs) of WSOC extracted from sand A (left) and sand B (right) from two sites in the Sahara Desert.

Discussion

Terrigenous inputs of dust and marine aerosols are the two most important global sources of aerosols, representing a combined 81% of global aerosol emissions (Schlesinger 1997), and the Sahara is the most dominant source (at >50%) of terrigenous dust (Schütz et al. 1981). Therefore, the inputs of dust and marine aerosol deposition to lakes should be significant, globally. Indeed, the effects of deposition of nutrients, in particular phosphate, and inorganic ions, such as calcium and iron, from Saharan dust have been observed in lakes and oceans (Duce and Tindale 1991; Morales-Baquero et al. 2006; Pulido-Villena et al. 2006). In this study, we show that Saharan dust also provides CDOM to an alpine lake and we provide new information regarding the specific chromophoric compounds that can be traced from deposition to the lake.

In the unvegetated, rocky catchment of La Caldera, atmospheric deposition represents the major input of soluble organic material. Our calculation that the dry and wet WSOC deposited in the lake and catchment over a 1-month period represented over 70% of the total lake DOC mass suggests that atmospheric deposition may have a very large influence over the distribution of organic compounds in the lake. Further, similarities in molar absorption and fluorescence between WSOC extracted

Table 5. Absorption and fluorescence properties of DOM from La Caldera from Aug–Oct 2007.

Properties*	La Caldera† (<i>n</i> = 16)	Soil near lake‡	Dust near lake
Absorption			
a_{250} (m^{-1})	2.22 (1.0–4.7)	14.4	7.6
a_{280} (m^{-1})	1.54 (0.6–3.0)	10.0	6.1
a_{320} (m^{-1})	0.83 (0.1–2.1)	4.8	3.8
ϵ_{250} ($\text{m}^2 \text{mmol}^{-1}$)	51 (4.4–175)	23	73
ϵ_{280} ($\text{m}^2 \text{mmol}^{-1}$)	35 (3.0–111)	16	59
ϵ_{320} ($\text{m}^2 \text{mmol}^{-1}$)	20 (1.2–71)	7.7	37
Fluorescence			
FI	1.59 (1.49–1.70)	1.75	1.39
Total loading (RU)	1.1 (0.57–1.95)	1.13	0.57
f_{total} (RU L mmol^{-1})	22 (2.6–44)	1.82	5.50
%C1	T	10	5.1
%C2 (Q2)	M	14	13
%C3	M	7.3	6.2
%C4 (HQ)	B	16	27
%C5 (SQ1)	T	0.8	3.8
%C6	M	6.1	1.1
%C7 (SQ2)	M	8.4	3.9
%C8 (Trp)	M	2.9	5.0
%C9 (SQ3)	M	3.3	5.1
%C10	T	3.1	5.4
%C11 (Q1)	T	4.1	4.3
%C12 (Q3)	M	12	11
%C13 (Tyr)	M	12	8.9
%AAs		15	14
RI	0.42 (0.37–0.47)	0.49	0.58

* FI, fluorescence index (dimensionless); f_{total} , total molar fluorescence; RI, redox index. The molecular association of components (Cory and McKnight 2005) is defined as: M, microbial; T, terrestrial; B, associated with both microbial and terrestrial DOM sources; Q, quinone-like; SQ, semiquinone-like; HQ, hydroquinone-like; Trp, tryptophan-like; Tyr, tyrosine-like; AAs, amino acid-like components (C8 + C13).

† Mean values listed with range (min–max) shown in parentheses. *n* = number of samples.

‡ PARAFAC fit was not suitable for this sample, and total loading, f_{total} , and the distribution of components are shown for comparison only.

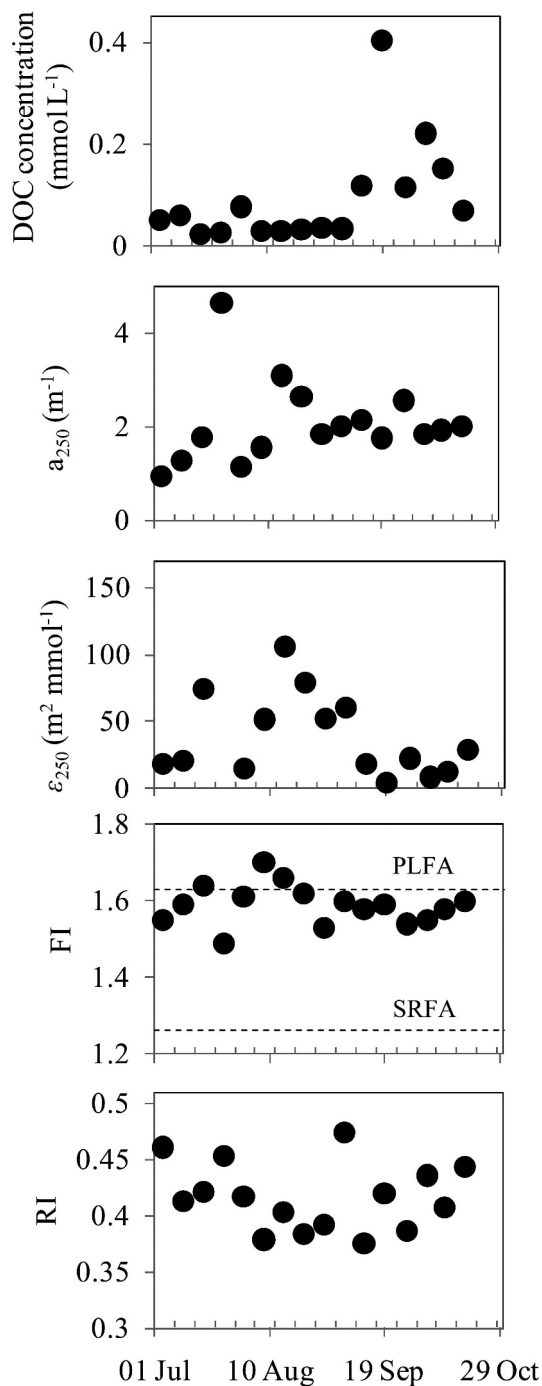


Fig. 5. Time series of DOC concentration, absorption coefficient at 250 nm (a_{250}), molar absorption coefficient at 250 nm (ϵ_{250}), fluorescence index (FI), and redox index (RI) in La Caldera. The FI values of microbial (Pony Lake Reference Fulvic Acid [PLFA]) and terrestrial (Suwannee River Reference Fulvic acid [SRFA]) end members are shown.

from dust collected in the catchment and both the lake and atmospheric deposition reinforce that the catchment acts to convey WSOC from atmospheric deposition to the lake. Unlike the dust collected in the catchment, WSOC from deeper soil was extremely different from lake WSOC,

showing lower total molar fluorescence and molar absorption than the lake.

The significant relationships for ϵ_{250} and ϵ_{280} between lake DOM and WSOC in total deposition further illustrate the importance of dust deposition for lake CDOM dynamics. The substantial changes that can be observed in the atmospheric dust concentrations from one day to the next (e.g., $0 \mu\text{g m}^{-3}$ on 23 August 2007 vs. $600 \mu\text{g m}^{-3}$ on 24 August 2007 at 3000 m asl) and the action of rain events, although less frequent than the constant dry deposition experienced in this region, to flush in organic aerosol deposition from the watershed may result in large variability in the amount of light-absorbing compounds in the lake on a daily timescale. Although we were able to observe significant relationships between lake and deposition optical properties, the temporal variability in amounts and types of deposition provides motivation for studying deposition effects over shorter timescales.

Another implication of significant relationships between molar absorption coefficients in the lake and in atmospheric deposition samples is that these optical properties can serve as tracers or fingerprints of dust deposition in the lake. Moreover, relationships between the PARAFAC components in lake and deposition samples revealed that a specific fluorophore could be traced to the lake from atmospheric deposition. Our results show that C9, a semiquinone-like component that was significantly related in the lake and in total deposition in terms of both its molar fluorescence and percentage of total fluorescence, could represent another fingerprint of organic material supplied to the lake by aerosol deposition.

During our collection period, the Sierra Nevada received dust mainly from Saharan and marine air masses, which is typical for the southwest Mediterranean region. The WSOC in deposition at this high elevation site was characterized by dynamic changes in absorbance and fluorescence among depositional periods (Table 1), probably resulting from these diverse sources, and is consistent with other studies (Duarte et al. 2005; Krivácsy et al. 2008) that have shown spatial and temporal variability in absorbance and fluorescence properties of organic aerosols. The diversity in chemical structure of organic aerosols observed in Krivácsy et al. (2008) supports our observations of two types of dry deposition periods, dominated by Saharan and marine air masses and reflected in two very different types of EEMs. In EEMs of Saharan-dominated WSOC, the characteristic fluorescent peaks attributed to humic substances and amino acids (Coble 1996) were present. PARAFAC analyses, showing that both terrestrial and microbial quinone-like components were abundant in Saharan-dominated WSOC, suggest that the organic material in dust includes both terrestrial and microbial precursor material, and a low FI in the WSOC favors lignaceous (plant or soil) sources.

Given the importance of Saharan dust export to this site, it was expected that WSOC from Saharan soil would contain similar fluorescence properties to WSOC from Saharan-dominated deposition. Instead, the Saharan soil WSOC had a very high FI, and PARAFAC analyses indicated that the EEM from this "end-member" environ-

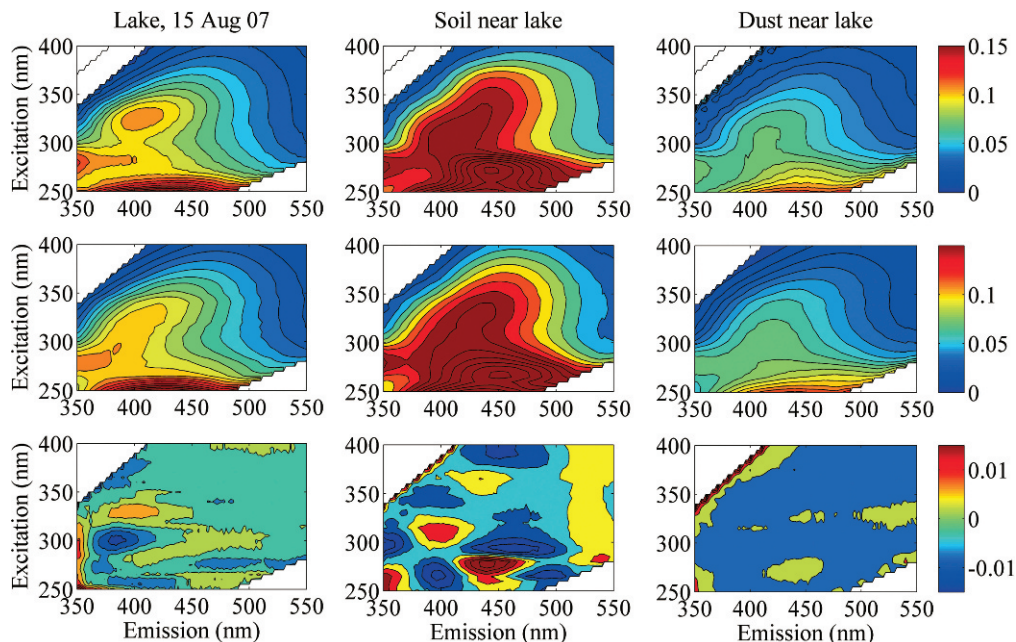


Fig. 6. Representative measured (top panels), PARAFAC-modeled (middle panels), and residual (bottom panels) excitation emission matrices (EEMs) of La Caldera lake water (left), a soil sample collected near the lake (center), and a sample of dust swept off rocks near the lake (right).

ment was dominated by amino acid-like components and contained almost no amount of C9 and little or no amount of components C5, C6, and C10. The implication of these results is that the semiquinone-like component C9 and other fluorescent compounds found in aerosol deposition are formed via aerosol transformations during transport in the atmosphere. This lack of some fluorescent components in Saharan soil WSOC that are present in deposition WSOC would suggest that Saharan mineral dust attracts organic compounds in the atmosphere and incorporates them into the particle phase during transport. However, Maria et al. (2004) suggest that organic compounds in African mineral dust particles are most likely associated with the dust source. Furthermore, considering the known

effects of UV light on humic DOM (Tranvik and Bertilsson 2001), we expect that UV light would photoreact with organic matter in the atmosphere, removing reduced quinones and chromophoric compounds, rather than producing them. In an experimental study by Gelencsér et al. (2003), loss of chromophoric compounds was observed when a representative continental aerosol solution was exposed to hydrogen peroxide to simulate atmospheric reactions of organic species with hydroxyl radicals. The initial absorbance of this solution was similar to what we show for the Saharan-dominated sample (Fig. 3A) but became featureless over time of the experiment. However, when the solution was exposed to sunlight, color returned in several days. These results suggest that the absorbance

Table 6. Mass balance calculation for DOC inputs from atmospheric deposition to La Caldera.

Property	Mean	Range
Lake catchment area (km ²)*	2.35×10^{-1}	—
Lake surface area (km ²)*	2.1×10^{-2}	—
Lake volume (L)	4.9×10^7	—
Lake DOC concentration (mmol L ⁻¹)	0.09	0.02–0.40
Lake DOC mass (mmol)	4.5×10^6	1.4×10^6 – 5.6×10^6
WSOC dry loading (mmol m ⁻² d ⁻¹)	0.29	0.20–0.42
WSOC wet loading (mmol m ⁻² d ⁻¹)	0.13	0.06–0.31
	Over 1 d	Over 30 d
WSOC dry deposition on lake (mmol)	6.1×10^3	1.8×10^5
WSOC wet deposition on lake (mmol)	2.8×10^3	0.8×10^5
WSOC dry deposition in catchment (mmol)	68×10^3	20×10^5
WSOC wet deposition in catchment (mmol)	31×10^3	9.3×10^5
Ratio of total daily WSOC deposition† to mean lake DOC mass (%)	2.4	72

* Source: Morales-Baquero et al. (2006).

† Combined dry and wet lake and catchment deposition.

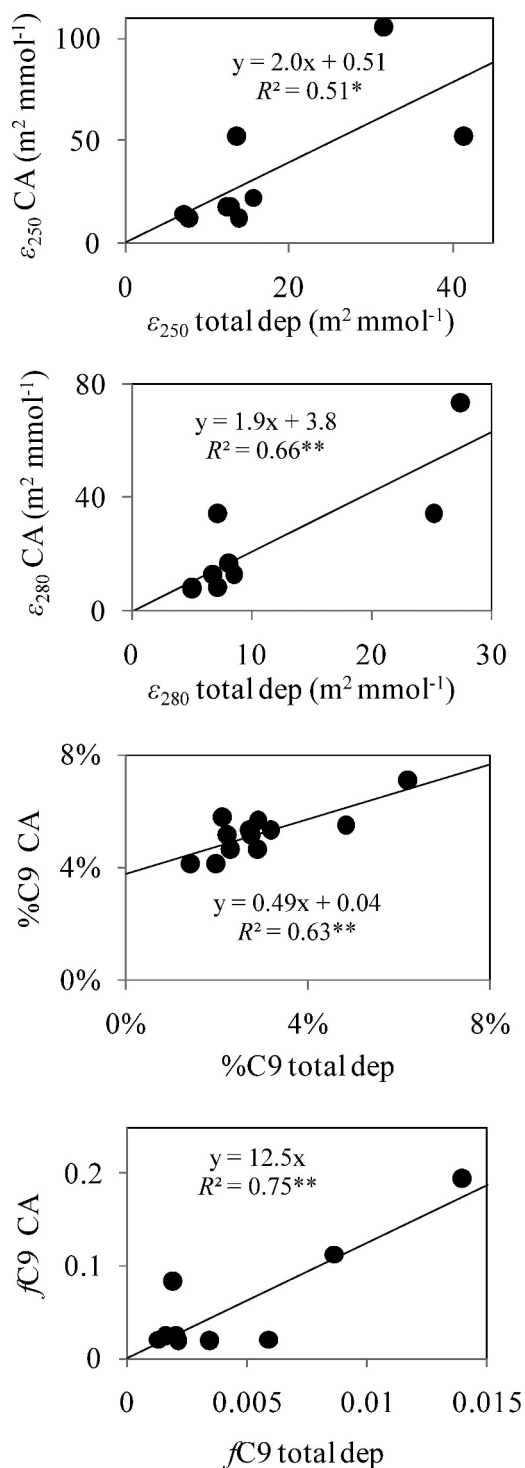


Fig. 7. Lake La Caldera (CA) and total (dry and wet) atmospheric deposition (total dep) relationships for molar absorption coefficients at 250 nm (ϵ_{250}) and 280 nm (ϵ_{280}), relative amount of component 9 (%C9), and molar fluorescence of C9 ($f \text{C9}$). * $p < 0.05$; ** $p < 0.01$.

and fluorescence spectra of organic aerosols can be greatly influenced by atmospheric photochemistry and their interpretation lies beyond simple end-member analysis. Nevertheless, the sources of organic matter in Saharan dust

deposition and the transformations that organic matter in dust may undergo during transport, including phototransformations, are questions that remain to be answered in future research.

The EEMs of marine-dominated WSOC were much different from EEMs of Saharan-dominated WSOC and from WSOC EEMs described elsewhere (Duarte et al. 2004; Kieber et al. 2006), with very low fluorescence intensity at higher excitation wavelengths (Fig. 3B) and a higher content of amino acid-like fluorescent components (Table 1). Given that the air masses bringing this deposition originate in the Atlantic Ocean, the organic compounds may be derived from amino acids found in marine aerosols and released by bubble-bursting processes (Jacobson et al. 2000). These EEMs are also quite different from EEMs of marine waters, such as those reported in Coble (1996). If organic aerosols traveling in marine air masses are associated with marine waters, then these differences may be due to processing in the atmosphere or aquatic production of organic material that cannot be lofted and transported as aerosol.

Our analyses of the WSOC in atmospheric deposition provide insights into the specific compounds that influence color in organic aerosols. The significant relationships between a_{320} in deposition WSOC and the content of semiquinone-like components (C7 and C9) and the anomeric-type component, C1, suggest that these compounds are responsible for color. C9 was also significantly related to a_{250} and a_{280} in total deposition, and C9, absorption, and molar absorption coefficients were higher in the Saharan-dominated deposition than marine-dominated deposition, suggesting that Saharan-derived air masses provide more chromophoric compounds. However, the mineralogical composition of dust, mostly iron oxides, can also affect these optical signatures (Linke et al. 2006). The significant negative relationships between amounts of amino acid-like fluorescent components (C8 + C13) and absorption coefficients (a_{250} , a_{320} , ϵ_{250} , and ϵ_{320}) indicate that as quinone-like and other fluorescent compounds become less abundant in aerosol deposition and the amount of amino acid-like fluorescence becomes more dominant in the EEMs, the aromaticity and color of WSOC decreases. In combination with the lower f_{total} of marine-derived WSOC, these results further suggest that marine aerosols are a source of more labile (amino acid-like) organic material that has substantially less color than organic material from Saharan aerosols. In comparison with WSOC of dry deposition, WSOC of wet deposition was characterized by molar absorption coefficients, f_{total} , and EEMs that were more similar to Saharan- than marine-derived dry deposition, with the exception of their higher amino acid-like fluorescence. Given that almost all of the rain events were associated with Saharan air masses and that rain contains large amounts of tyrosine- and tryptophan-like fluorescent compounds (Muller et al. 2008), this combination of highly colored and fluorescent material that also contains large amounts of amino acid-like fluorescence is not an expected result.

Nevertheless, our findings that atmospheric deposition reflected fluorescence properties of both quinone-like and

amino acid-like humic material is relevant in terms of the many functions of these compounds in aquatic environments. Whereas labile amino acid-like DOM may represent an energy source for bacteria, the light-absorbing quality of chromophoric compounds provides essential UV protection for lake bacterioplankton (Alonso-Saez et al. 2006) and is especially important in alpine lakes that are vulnerable to UV radiation.

Although the effects of UV radiation are regulated by CDOM in alpine lakes (Laurion et al. 2000), UV radiation also acts to transform DOM in La Caldera (Reche et al. 2001), as reflected in its fluorescence properties. The EEMs of La Caldera contained prominent peaks located at Ex:Em of 240:420 nm and 313:405, resembling those of EEMs of microbially derived fulvic acids because of their position at low-emission wavelengths (McKnight et al. 2001). Although bacterial and algal exudates represent important sources of DOM in alpine lakes, this blue-shifting (to low-emission wavelengths) of the dominant peaks may also be attributed to a loss of fluorescent components and longer wavelength chromophores, resulting from photobleaching (Gibson et al. 2001; Reche et al. 2001). We also noted the occurrence of a narrower region of fluorescence centered at Ex:Em 300:380 nm in the measured lake EEMs than in the PARAFAC-modeled EEMs, resulting in a residual peak at this location that was not due to sampling or handling effects. Instead, the presence of this residual peak suggests some fundamental difference in the fluorescent compounds of alpine lakes vs. the lower elevation sample set used in the Cory and McKnight (2005) PARAFAC model. Potential effects of UV light and other extreme conditions on the structure of fluorescent compounds warrants further investigation.

In this study, we showed that WSOC from atmospheric deposition provided substantial amounts of DOM to La Caldera, an alpine lake in the Sierra Nevada, Spain. Moreover, we found that the synchronous changes in absorbance and fluorescence of dry-deposition WSOC and lake DOM provide an avenue for examining the effects of aerosol deposition on the chemical quality of alpine lakes. We showed that the chemical character of WSOC was dynamic and related to the source of air masses, with Saharan and marine-dominated deposition exhibiting two very different types of spectroscopic properties. These differences between organic aerosol sources support the notion that marine aerosols provide little color to alpine lakes, whereas Saharan dust represents the main source of CDOM to alpine lakes. Then, DOM absorbance and fluorescence in alpine lakes such as La Caldera may be useful sentinels of increased dust transport due to desertification and climate change (Schindler 2009). Given the photoprotective role of CDOM in lakes, the projected increases in global dust transport (Prospero and Lamb 2003) may have a positive feedback on alpine lake microbiota.

Acknowledgments

We thank T. Serrano, I. Perez Mazuecos, R. Morales-Baquero, and R. McGrath, who helped with sample collection and processing. We are grateful to J. C. Brito for collecting the

Saharan soil samples for this study and to L. Alados-Arboledas and F. J. Olmo for insights regarding aerosol deposition sources. We also thank the anonymous reviewers who helped to greatly improve this manuscript. The authors gratefully acknowledge the National Oceanic and Atmospheric Administration (NOAA) Air Resources Laboratory for use of the HYbrid Single-Particle Lagrangian Integrated Trajectory (HYSPLIT) model and Real-time Environmental Applications and Display sYstem (READY) website, the NOAA National Data Center Climate Data Online, the Barcelona Supercomputing Center (BSC) for the use of vertical dust profile data from the Dust Regional Atmospheric Model, and the Ministerio de Medio Ambiente and Medio Rural y Marino, the Consejo Superior de Investigaciones Científicas, and the Agencia Estatal de Meteorología of Spain for the use of atmospheric pollution data from the Calima project. We are grateful to the Sierra Nevada National Park Office for providing access and to the staff of the Observatorio de Sierra Nevada (Instituto de Astrofísica de Andalucía, Consejo Superior de Investigaciones Científicas, Granada, Spain) for their support with atmospheric deposition samplers.

Funding was provided by Fundación Banco Bilbao Vizcaya-Argentaria (BIOCON04/009), Junta de Andalucía (P06-RNM-01503), and Ministerio de Medio Ambiente (080-2007).

References

- ALONSO-SAEZ, L., J. M. GASOL, T. LEFORT, J. HOFER, AND R. SOMMARUGA. 2006. Effect of natural sunlight on bacterial activity and differential sensitivity of natural bacterioplankton groups in northwestern Mediterranean coastal waters. *Appl. Environ. Microbiol.* **72**: 5806–5813.
- BANAITIS, M. R., H. WALDRIP-DAIL, M. S. DIEHL, B. C. HOLMES, J. F. HUNT, R. P. LYNCH, AND T. OHNO. 2006. Investigating sorption-driven dissolved organic matter fractionation by multidimensional fluorescence spectroscopy and PARAFAC. *J. Colloid Interface Sci.* **304**: 271–276.
- BARON, J. S., H. M. RUETH, A. M. WOLFE, K. R. NYDICK, E. J. ALLSTOTT, J. T. MINEAR, AND B. MORASKA. 2000. Ecosystem responses to nitrogen deposition in the Colorado Front Range. *Ecosystems* **3**: 352–368, doi: 10.1007/s100210000032.
- CHIN, Y., G. AIKEN, AND E. O'LOUGHLIN. 1994. Molecular weight, polydispersivity and spectroscopic properties of aquatic humic substances. *Environ. Sci. Technol.* **28**: 1853–1858.
- COBLE, P. G. 1996. Characterization of marine and terrestrial DOM in seawater using excitation-emission matrix spectroscopy. *Mar. Chem.* **51**: 325–346.
- CORY, R. M., AND D. M. MCKNIGHT. 2005. Fluorescence spectroscopy reveals ubiquitous presence of oxidized and reduced quinones in dissolved organic matter. *Environ. Sci. Technol.* **39**: 8142–8149.
- DRAXLER, R. R., AND G. D. ROLPH. 2003. HYSPLIT (HYbrid Single-Particle Lagrangian Integrated Trajectory) model access via NOAA ARL READY website (<http://www.arl.noaa.gov/ready/hysplit4.html>). NOAA Air Resources Laboratory.
- DUARTE, R.M.B.O., C. A. PIO, AND A. C. DUARTE. 2004. Synchronous scan and excitation-emission matrix fluorescence spectroscopy of water-soluble organic compounds in atmospheric aerosols. *J. Atmos. Chem.* **48**: 157–171.
- , ———, AND ———. 2005. Spectroscopic study of the water-soluble organic matter isolated from atmospheric aerosols collected under different atmospheric conditions. *Anal. Chim. Acta.* **530**: 7–14.
- DUCE, R. A., AND N. W. TINDALE. 1991. Atmospheric transport of iron and its deposition in the ocean. *Limnol. Oceanogr.* **36**: 1715–1726.

- GELENCSE, A., A. HOFFER, G. KISS, R. KURDI, AND L. BENCZE. 2003. *In-situ* formation of light-absorbing organic matter in cloud water. *J. Atmos. Chem.* **45**: 25–33.
- GIBSON, J. A. E., W. F. VINCENT, AND R. PIENITZ. 2001. Hydrologic control and diurnal photobleaching of CDOM in a subarctic lake. *Arch. Hydrobiol.* **152**: 143–159.
- HEIRI, O., A. F. LOTTER, AND G. LEMCKE. 2001. Loss on ignition as a method for estimating organic and carbonate content in sediments: Reproducibility and comparability of results. *J. Paleolimnol.* **25**: 101–110.
- HOOD, E., D. M. MCKNIGHT, AND M. W. WILLIAMS. 2003. Sources and chemical character of dissolved organic carbon across an alpine/subalpine ecotone, Green Lakes Valley, Colorado Front Range, United States. *Water Resour. Res.* **39**: 1188, doi: 10.1029/2002WR001738.
- JACOBSON, M. C., H. C. HANSSON, K. J. NOONE, AND R. J. CHARLSON. 2000. Organic atmospheric aerosols: Review and state of the science. *Rev. Geophys.* **38**: 267–294.
- KALBITZ, K., J. SCHMERWITZ, D. SCHWESIG, AND E. MATZNER. 2003. Biodegradation of soil-derived dissolved organic matter as related to its properties. *Geoderma* **113**: 273–291.
- KIEBER, R. J., R. F. WHITEHEAD, S. N. REID, J. D. WILLEY, AND P. J. SEATON. 2006. Chromophoric dissolved organic matter (CDOM) in rainwater, southeastern North Carolina, USA. *J. Atmos. Chem.* **54**: 21–41, doi: 10.1007/s10874-005-9008-4.
- KRIVÁCSY, Z., G. KISS, D. CEBURNIS, G. JENNINGS, W. MAENHAUT, I. SALMA, AND D. SHOOTER. 2008. Study of water-soluble atmospheric humic matter in urban and marine environments. *Atmos. Res.* **87**: 1–12.
- LAURION, I., M. VENTURA, J. CATALAN, R. PSENNER, AND R. SOMMARUGA. 2000. Attenuation of ultraviolet radiation in mountain lakes: Factors controlling the among- and within-lake variability. *Limnol. Oceanogr.* **45**: 1274–1288.
- LINKE, C., O. MOHLER, A. VERES, A. MOHACSI, Z. BOZOKI, G. SZABO, AND M. SCHNAITER. 2006. Optical properties and mineralogical composition of different Saharan mineral dust samples: A laboratory study. *Atmos. Chem. Phys.* **6**: 3315–3323.
- MARIA, S. F., L. M. RUSSELL, M. K. GILLES, AND S. C. B. MYNENI. 2004. Organic aerosol growth mechanisms and their climate-forcing implications. *Science* **306**: 1921–1924, doi: 10.1126/science.1103491.
- MCKNIGHT, D. M., E. W. BOYER, P. K. WESTERHOFF, P. T. DORAN, T. KULBE, AND D. T. ANDERSEN. 2001. Spectrofluorometric characterization of dissolved organic matter for indication of precursor organic material and aromaticity. *Limnol. Oceanogr.* **46**: 38–48.
- MILLER, M. P., D. M. MCKNIGHT, R. M. CORY, AND M. W. WILLIAMS. 2006. Hyporheic exchange and humic redox reactions in an alpine stream/wetland ecosystem, Colorado Front Range. *Environ. Sci. Technol.* **40**: 5943–5949.
- MLADENOV, N., P. HUNTSMAN-MAPILA, P. WOLSKI, W. R. L. MASAMBA, AND D. M. MCKNIGHT. 2008. Dissolved organic matter accumulation, reactivity, and redox state in ground-water of a recharge wetland. *Wetlands* **28**: 747–759.
- , D. M. MCKNIGHT, S. A. MACKO, R. M. CORY, M. NORRIS, AND L. RAMBERG. 2007. Chemical characterization of DOM in channels of a seasonal wetland. *Aquat. Sci.* **69**: 456–471.
- , E. PULIDO-VILLENA, R. MORALES-BAQUERO, E. ORTEGA-RETUERTA, R. SOMMARUGA, AND I. RECHE. 2008. Spatio-temporal drivers of dissolved organic matter in high alpine lakes: The role of Saharan dust inputs and bacterial activity. *J. Geophys. Res.* **113**: G00D01, doi: 10.1029/2008JG000699.
- MORALES-BAQUERO, R., E. PULIDO-VILLENA, AND I. RECHE. 2006. Atmospheric inputs of phosphorus and nitrogen to the southwest Mediterranean region: Biogeochemical responses of high mountain lakes. *Limnol. Oceanogr.* **51**: 830–837.
- MORRIS, D. P., H. ZAGARESE, C. E. WILLIAMSON, E. G. BALSEIRO, B. R. HARGREAVES, B. MODENUTI, AND C. QUEIMALIÑOS. 1995. The attenuation of solar UV radiation in lakes and the role of dissolved organic carbon. *Limnol. Oceanogr.* **40**: 1381–1391.
- MOULIN, C., AND I. CHIAPELLO. 2006. Impact of human-induced desertification on the intensification of Sahel dust emission and export over the last decades. *Geophys. Res. Lett.* **33**: L18808, doi: 10.1029/2006GL025923.
- MULLER, C., A. BAKER, R. HUTCHINSON, I. J. FAIRCHILD, AND C. KIDD. 2008. Analysis of rainwater dissolved organic carbon compounds using fluorescence spectrophotometry. *Atm. Environ.* **42**: 8036–8045.
- NEFF, J. C., AND OTHERS. 2008. Increasing eolian dust deposition in the western United States linked to human activity. *Nature Geosci.* **1**: 189–195, doi: 10.1038/ngeo133.
- PROSPERO, J. M., AND P. J. LAMB. 2003. African droughts and dust transport to the Caribbean: Climate change implications. *Science* **302**: 1024–1027, doi: 10.1126/science.1089915.
- PULIDO-VILLENA, E., I. RECHE, AND R. MORALES-BAQUERO. 2005. Food web reliance on allochthonous carbon in two high mountain lakes with contrasting catchments: A stable isotope approach. *Can. J. Fish. Aquat. Sci.* **62**: 2640–2648.
- , ———, AND ———. 2006. Significance of atmospheric inputs of calcium over the southwestern Mediterranean region: High mountain lakes as tools for detection. *Global Biogeochem. Cycles* **20**: GB2012, doi: 10.1029/2005GB002662.
- , ———, AND ———. 2008. Evidence of an atmospheric forcing on bacterioplankton and phytoplankton dynamics in a high mountain lake. *Aquat. Sci.* **70**: 1–9, doi: 10.1007/s00027-007-0944-8.
- RECHE, I., E. ORTEGA-RETUERTA, O. ROMERA, E. PULIDO-VILLENA, R. MORALES-BAQUERO, AND E. O. CASAMAYOR. 2009. Effect of Saharan dust inputs on bacterial activity and community composition in Mediterranean lakes and reservoirs. *Limnol. Oceanogr.* **54**: 869–879.
- , E. PULIDO-VILLENA, J. M. CONDE-PORCUNA, AND P. CARRILLO. 2001. Photoreactivity of dissolved organic matter from high-mountain lakes of Sierra Nevada, Spain. *Arct. Antarct. Alp. Res.* **33**: 426–434.
- SCHINDLER, D. W. 2009. Lakes as sentinels and integrators for the effects of climate change on watersheds, airsheds, and landscapes. *Limnol. Oceanogr.* **54**: 2349–2358.
- SCHLESINGER, W. H. 1997. *Biogeochemistry: An analysis of global change*, 2nd ed. Academic.
- SCHÜTZ, L., R. JAENICKE, AND H. PIETREK. 1981. Saharan dust transport over the North Atlantic Ocean, p. 87–100. *In* T. L. Péwé [ed.], *Desert dust: Origin, characteristics, and effects on man*. Geological Society of America, Special Paper 186.
- SOMMARUGA, R., I. OBERNOSTERER, G. J. HERNDL, AND R. PSENNER. 1997. Inhibitory effect of solar radiation on thymidine and leucine incorporation by freshwater and marine bacterioplankton. *Appl. Environ. Microbiol.* **63**: 4178–4184.
- STEDMON, C. A., S. MARKAGER, AND R. BRO. 2003. Tracing dissolved organic matter in aquatic environments using a new approach to fluorescence spectroscopy. *Mar. Chem.* **82**: 239–254.
- TRANVIK, L. J., AND S. BERTILSSON. 2001. Contrasting effects of solar UV radiation on dissolved organic sources for bacterial growth. *Ecol. Lett.* **4**: 458–463.
- WEDBORG, M., T. PERSSON, AND T. LARSSON. 2007. On the distribution of UV-blue fluorescent organic matter in the Southern Ocean. *Deep-Sea Res.* **54**: 1957–1971.

WEISHAAR, J. L., G. R. AIKEN, B. A. BERGAMASCHI, M. S. FRAM, R. FUJII, AND K. MOPPER. 2003. Evaluation of specific ultraviolet absorbance as an indicator of the chemical composition and reactivity of dissolved organic carbon. *Environ. Sci. Technol.* **37**: 4702–4708.

Associate editors: Warwick F. Vincent and John P. Smol

Received: 12 September 2008

Accepted: 15 April 2009

Amended: 15 May 2009